Anomalous physical transport in complex networks

Christos Nicolaides, Luis Cueto-Felgueroso, and Ruben Juanes*

Massachusetts Institute of Technology, 77 Massachusetts Avenue, Building 48-319, Cambridge, Massachusetts 02139, USA
(Received 15 June 2010; revised manuscript received 8 October 2010; published 10 November 2010)

The emergence of scaling in transport through interconnected systems is a consequence of the topological structure of the network and the physical mechanisms underlying the transport dynamics. We study transport by advection and diffusion in scale-free and Erdős-Rényi networks. Velocity distributions derived from a flow potential exhibit power-law scaling with exponent $\nu \approx \gamma+1$, where γ is the exponent of network connectivity. Using stochastic particle simulations, we find anomalous (nonlinear) scaling of the mean-square displacement with time. We show the connection with existing descriptions of anomalous transport in disordered systems, and explain the mean transport behavior from the coupled nature of particle jump lengths and transition times.

An overarching challenge in network science is the study of the dynamics of processes that take place on complex networks, which describe the topology of many interconnected systems in nature and society [1–5]. Network theory provides a framework to understand—and possibly optimize and control—dynamic phenomena as diverse as data exchange [6], epidemics and spreading of mobile agents [7], fluxes in metabolic networks [8,9], or the spatial dynamics of humans and goods through transportation systems [10,11].

Recent work has led to fundamental advances in our understanding of flow and transport properties of complex networks. These include the analysis of the conductance between two arbitrarily chosen nodes in scale-free or Erdős and Rényi (E-R) networks [12]—an analysis that has been extended to the case of multiple sources and sinks [13,14] and to weighted networks [15]. The dynamics of spreading through scale-free networks have been studied by means of *diffusive* random walks [9,16–19], which have led to scalings for the mean first passage time (MFPT) in terms of network centrality [16] and modularity [9]. Studies to date leave open, however, the question of how *directional bias* impacts transport. Bias or drift occurs naturally in many network systems, including advection from a flow potential [12], agent spreading in topologies with sources and sinks, such as utility networks [20] and freely diffusing molecules in tissue [21], and tracer diffusion in suspensions of swimming microorganisms [22].

Here, we study the scaling properties of physical transport in scale-free and Erdős-Rényi networks. The fundamental question is whether the topology of the network, the underlying physical mechanisms, or both, control the scaling properties of transport in complex networks. Transport is physical in the sense that, as observed in most natural settings, the spreading process is conservative and driven by the interplay between advection—which derives from a flow potential—and diffusion, which we model through random walks. We show that advection leads to anomalous (non-Fickian) transport, as evidenced by the nonlinear time scaling of the mean-square displacement (MSD) of tracer particles migrating through the network. The simulation results suggest that a mean-field theory such as continuous time random walk

(CTRW), which describes transport from a joint probability distribution of particle jump lengths and transition times [23–26], may be used to capture the average transport behavior. We show that coupling between space and time [27,28] is essential to describe advective transport in a complex network.

We construct scale-free networks, characterized by a power-law connectivity distribution, $P(k) \sim k^{-\gamma}$, where k is the number of links attached to a node and γ is the characteristic exponent of the network, with $2 \leq \gamma \leq 4.8$. We generate graphs following the Molloy-Reed scheme [29]. Given the size of the network (N nodes), the degree exponent γ, and fixing the minimum degree to be $k_{\min}=2$, we use the relations from Aiello *et al.* [30] to obtain the degree sequence from a power-law distribution. We then produce a list of k_i copies of each node i and attach links between nodes by randomly pairing up elements of this list until none remain. We disallow double links, as well as self-linked nodes. This algorithm generates networks of excellent accuracy for arbitrary exponents γ even for relatively small network sizes. We generate an Erdős-Rényi network by attaching a link to each pair of nodes with probability $p=0.01$. We assume for simplicity that the nodes in our model network are uniformly spaced in the unit square (Fig. 1). The positioning of nodes on a square lattice is an idealization of networks with spatial
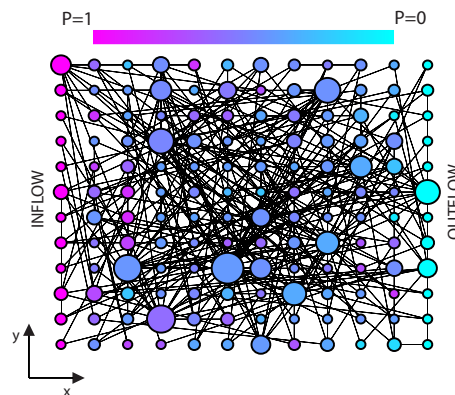

FIG. 1. (Color online) Schematic representation of our model network. Nodes are distributed uniformly on the unit square. Their connectivity (represented by node diameter) follows a power-law distribution. Flow through the network derives from a potential P that varies between 1 (left boundary) and 0 (right boundary).
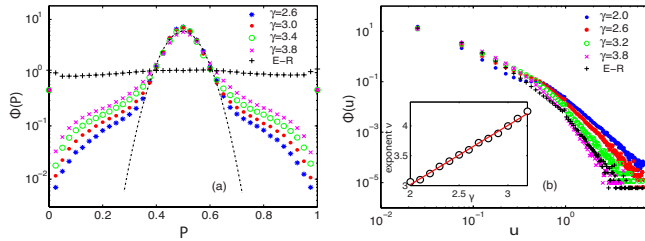
*juanes@mit.edu

FIG. 2. (Color online) (a) Pressure distributions, $\Phi(P)$, for scale-free networks with different degree exponents, γ, as well as for an E-R network. The dashed line is a Gaussian fit with mean $\bar{P}=0.5$ and standard deviation $\sigma_P \approx 0.08$. We use networks of size $N=8100$ nodes, and the results are averaged over 250 realizations. (b) Velocity distributions, $\Phi(u)$, for different network types. Inset: exponent ν of the velocity distribution power-law tail plotted against the connectivity exponent $\gamma \in [2,3.2]$; shown also is a least-squares linear interpolation $\nu = (0.99 \pm 0.02)\gamma + (1.03 \pm 0.05)$.

embedding that exhibit power-law connectivity, including power and distribution networks [20] and transportation and biological systems [31]. Networks embedded in metric spaces often exhibit a decay of nodal connectivity with distance [32,33]—we have not included this distance-dependent connectivity in our study which therefore allows for long-ranged links.

Flow through the network is driven by a scalar (potential) field and satisfies conservation of mass. At every node i we impose $\Sigma_j u_{ij}=0$, where u_{ij} is the flux through the link connecting nodes i and j. The fluxes are given by

$$u_{ij} = -\lambda_{ij}\frac{P_i - P_j}{d_{ij}}, \qquad (1)$$

where P_i and P_j are the flow potentials at nodes i and j, respectively, and d_{ij} is the Euclidean distance between the two nodes. This problem is exactly analogous to the electric conductance model of [12–15], except that in our model the relation between velocity and potential difference is modulated by the inverse of link length. Here, we assume that the conductivity is the same for all links and takes a value $\lambda_{ij}=1$. To elucidate the essential mechanisms governing transport, we study a simple setting of flow from left to right by fixing the potential $P=1$ at the inflow nodes (left boundary), and $P=0$ at the outflow nodes (right boundary). Flow is confined between the top and bottom boundaries. Inserting the flux equation [Eq. (1)] into the mass conservation condition at each node, and imposing the boundary conditions, leads to a linear system of algebraic equations to be solved for the flow potential at the nodes, $\{P_j\}$, which are stationary and do not evolve in time. This system of equations is solved with a direct solution method such as Gaussian elimination.

For different values of the degree exponent γ, the distributions of nodal potential collapse in the range $P \in (0.4,0.6)$ [Fig. 2(a)]. Within this range, the flow potential seems to be normally distributed (dashed line). The velocity at the links, u, follows a distribution that exhibits a power-law tail [Fig. 2(b)]. In the range $\gamma \in [2,3.2]$, the exponent of the velocity power-law distribution is well approximated as $\nu \approx \gamma+1$ [Fig. 2(b), inset]. As a consequence of this behavior,

a slower decay in network connectivity (smaller γ) results in increased probability of observing large velocities at the links. Interestingly, the flow potential distribution for a random (Erdős-Rényi) network has a very different shape from that of scale-free networks, yet it also leads to a power-law tail distribution of the link velocities. Note that for a regular lattice, the distribution of flow potentials is uniform, and the distribution of velocities is a double Dirac delta function.

We investigate the scaling properties of transport in scale-free networks through stochastic particle simulations. This allows us to explore the transition between the purely diffusive and advective regimes. Particles move along the links of the network according to the local advective velocity field obtained from the steady-state potential solution, together with an additional random diffusive component sampled from a Gaussian distribution:

$$X_{N+1} = X_N + \delta X_N, \qquad (2)$$

$$\delta X_N = u_{ij}\delta t + \sqrt{2D\delta t}\,\xi, \qquad (3)$$

$$X_{N+1} \geq 0, \qquad (4)$$

where X denotes the coordinate along the link, D is the diffusion coefficient, and $\xi = N(0,1)$. At $t=0$, we inject particles at random at the inflow nodes. A particle located at node i at a given time step chooses one of the *outgoing* links to "walk" on it. Link selection is performed at random, with probability that is linearly proportional to the magnitude of the link velocity. The term outgoing refers here to links with velocity vectors pointing from the initial position of the particle (node i), to the destination connected nodes. Constraint Eq. (4) forces particles walking on a link ij to stay on it until they reach the destination node j. Particles are removed when they reach the outflow nodes.

The key parameter in this stochastic process is the ratio between advective and diffusive jump lengths, $A = \frac{\bar{u}\delta t}{\sqrt{2D\delta t}}$, where $\bar{u}$ is the characteristic velocity at the links. This computational quantity plays the role of the Péclet number (Pe $=\bar{u}\bar{d}/D$) in physical fluid flow, where $\bar{d}$ is the characteristic length of the links. The purely advective and diffusive limits correspond to $A \to \infty$ and $A=0$, respectively. A second computational parameter is $\varepsilon = \bar{u}\delta t/(A\bar{d})$, which measures the effect of the boundary constraint Eq. (4). By fixing the value of ε, we impose a constant ratio between the number of advective jumps affected by the constraint, and the average number of jumps needed for a particle to move from one node to another. This permits a rigorous interpretation of the results from particle tracking simulations. We analyze the Euclidean MSD, also known as dispersion, or variance of the particle plume, in the direction of the mean flow: $\langle \Delta x^2(t) \rangle = \langle x^2(t) \rangle - \langle x(t) \rangle^2$, where $\langle \cdot \rangle$ denotes averaging over all the particles.

In the advective limit ($A \gg 1$, $\varepsilon \ll 1$), the MSD follows a power law at early times, $\langle \Delta x^2(t) \rangle \sim t^\beta$, and then saturates due to finite size effects (Fig. 3, inset). We compute the scaling exponent β in the preasymptotic regime for scale-free networks with different exponents γ, as well as for an E-R network. Our simulations show that advection-dominated transport on scale-free networks is anomalous and exhibits
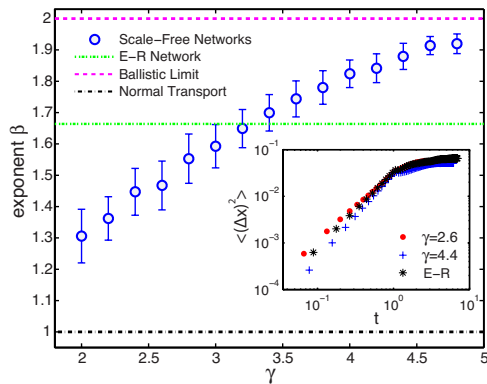
FIG. 3. (Color online) The particle MSD follows a power law in time during early times, before it is influenced by boundary effects (inset). The main plot shows the scaling exponent β of the particle MSD, for advection-dominated transport ($A \gg 1$) in scale-free networks, plotted against the connectivity degree exponent γ. Transport is anomalous and falls in the superdiffusive regime ($\beta > 1$). Shown also are the values of β for an E-R network—for which transport is also superdiffusive—and a regular lattice–for which transport is normal, $\beta = 1$. We use networks with $N = 8100$ nodes and set $A = 7$ and $\varepsilon = 0.0014$. We use 3000 particles and we average over 100 realizations. Within each realization, we construct the network, solve the flow potential equation, and advance particles by advection and diffusion, according to the flow field from the potential solution. This makes our model significantly more computationally expensive than the diffusive random-walk algorithms of [17,18], in which a walker jumps directly from node to node. We have confirmed that our results are independent of network size for $N > 6000$.

superdiffusive behavior, $\beta > 1$ (Fig. 3). The exponent β increases monotonically with γ. For large γ, it asymptotically reaches the ballistic limit, $\beta = 2$.

The scaling properties of transport in scale-free networks depend on the relative dominance between advective and diffusive mechanisms (Fig. 4). We perform simulations varying the ratio between the advective and diffusive jump lengths by controlling the value of parameter A. For small values of A, transport is governed by diffusion, while for large values advection dominates. The scaling exponent of the MSD increases monotonically with A. This implies a transition from the normal scaling ($\beta = 1$) of purely diffusive transport, to anomalous scaling ($\beta > 1$) in the advection-dominated limit. The asymptotic value of β as $A \to \infty$ is controlled by the topology of the network (Fig. 3).

The observed scaling can be understood within the CTRW framework [23,24,34]. The problem setup is essentially one-dimensional (1D) because flow is from left to right, so the key question is to ascertain how the topology of the network affects spreading in the direction of mean flow. CTRW assumes that the statistics of particle spreading can be fully characterized by a joint probability distribution, $\psi(\chi, \tau)$, of particle jump lengths, χ, and waiting time between jumps, τ, whose marginal distributions $\lambda(\chi)$ and $w(\tau)$, respectively, can be derived by integration. It is well understood that broad distributions of jump lengths or transition times may lead to anomalous transport [23,24,34]. To test the ability of CTRW to describe transport in scale-free networks, we per-
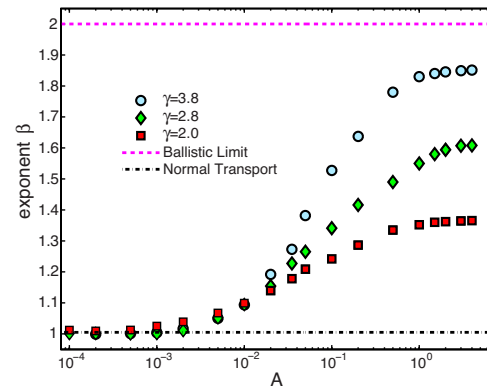

FIG. 4. (Color online) Purely diffusive transport ($A \ll 1$) in scale-free networks leads to linear scaling of the mean-square displacement ($\beta \approx 1$). As A increases, we observe a transition from normal transport to anomalous transport, with scaling exponents, β, that reach different asymptotic values in the superdiffusive regime, depending on the network topology (Fig. 3). We use networks with $N = 8100$ nodes, fixed $\varepsilon = 0.04$, and 3000 particles. Simulation results are averaged over 100 realizations.

form 1D random walks by sampling the empirical joint distributions $\psi(\chi, \tau)$ recorded from our network simulations. In the advection limit, the jump length can be represented by the length of the link, d. Since the network is restricted to a finite domain, d is bounded and is found to be well approximated by a Kumaraswamy distribution. In contrast—and due
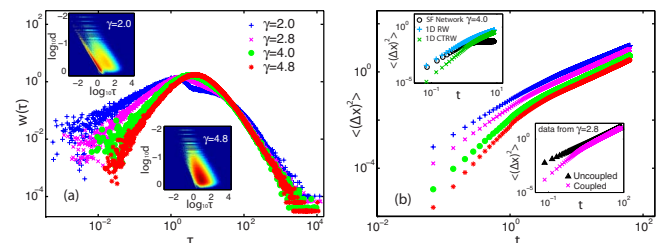

FIG. 5. (Color online) (a) Marginal distribution of waiting times for advection-dominated transport and different scale-free networks. Insets: joint distribution $\psi(d, \tau)$ for two different scale-free networks ($\gamma = 2.0$ and 4.8). Bright red color corresponds to high value of $\psi(d, \tau)$. Link length and transition time exhibit strong coupling for $\gamma = 2.0$, for which the joint distribution collapses around the scaling $\tau \sim d^2$. The results are for network size $N = 8100$ nodes and over 300 realizations. (b) MSD for coupled and unidirectional CTRW, using data from different network types. Bottom-right inset: MSD for coupled and uncoupled biased, 1D CTRW. Top-left inset: MSD from network simulations compared with the results from 1D coupled CTRW, and 1D RW with back-flow and linear interpolation along the jumps. By *backflow* we mean that the velocity along links in the network simulations is predominantly in the positive x direction, but the flow is "backward" for some links. The 1D random-walk simulations with backflow are based on taking a fraction of the jumps in the negative x direction, to better approximate the actual 2D network simulations. In the classical CTRW framework, particles are assumed to 'wait' at a given location until they jump to a new one. By *interpolation* we mean that we post-compute the MSD at a given time as if the particles had experienced a constant velocity between jumps—a behavior that more closely resembles the setting of the 2D particle tracking network simulations.

to the broad-ranged velocity distributions—the transition times between connected nodes, $\tau = d/u$, exhibit a wide range distribution with power-law tail, $w(\tau) \sim \tau^{-(1+\delta)}$ [Fig. 5(a)], where $\delta \approx 1.9$ for all degree exponents γ. In the case of decoupled CTRW [$\psi(\chi, \tau) = \lambda(\chi) w(\tau)$] in an infinite lattice under a bias, we would expect an asymptotic late-time scaling of the MSD, $\langle \Delta x^2(t) \rangle \sim t^{1.1}$ [24,26,35], in contrast with the observed scalings (Fig. 3) [36]. The lack of quantitative agreement between decoupled CTRW and the scaling observed in our network simulations highlights the importance of the coupling between jump length and waiting time [Fig. 5(a), insets] in the MSD, especially at early times [Fig. 5(b), bottom-right inset]. A 1D coupled CTRW qualitatively recovers the monotonic increasing trend of the scaling exponent β as a function of γ [Fig. 5(b)]. Quantitative agreement requires introducing additional information from the network simulations, such as the possibility of backflow, and linear interpolation of the particle positions between jumps [Fig. 5(b), top-left inset]. The transition to normal transport for small γ (Fig. 3) is consistent with the convergence of the joint distribution of jump lengths and transition times toward the geometric limit $\tau \sim d^2$ [Fig. 5(a), top-left inset]. This un-expected diffusionlike scaling, whose origin appears to lie in the existence of very well connected nodes, is responsible for bounding anomalous transport behavior.

The nonlinear scaling of spreading with time suggests that transport processes in complex networks are much faster than previously estimated using purely diffusive random walk models that neglect advective fluxes. In the presence of advection, the topology of the network plays a central role in the spreading dynamics, while for diffusion-dominated processes the scaling of spreading with time is independent of network connectivity. Our interpretation in terms of transition times links transport in complex networks with well-established models of effective transport through disordered systems, and opens the door to aggregate conceptualizations of biased transport processes in scale-free networks.

[1] A.-L. Barabási and R. Albert, Science **286**, 509 (1999).

[2] L. A. N. Amaral, A. Scala, M. Berthélémy, and H. E. Stanley, Proc. Natl. Acad. Sci. U.S.A. **97**, 11149 (2000).

[3] R. Albert and A.-L. Barabási, Rev. Mod. Phys. **74**, 47 (2002).

[4] M. C. González, H. J. Herrmann, J. Kertész, and T. Vicsek, Physica A **379**, 307 (2007).

[5] H. Jeong, B. Tombor, R. Albert, Z. N. Oltvai, and A.-L. Barabási, Nature (London) **407**, 651 (2000).

[6] K.-I. Goh, B. Kahng, and D. Kim, Phys. Rev. Lett. **87**, 278701 (2001).

[7] R. Pastor-Satorras and A. Vespignani, Phys. Rev. Lett. **86**, 3200 (2001).

[8] E. Almaas, B. Kovács, T. Vicsekand, Z. N. Oltvai, and A.-L. Barabási, Nature (London) **427**, 839 (2004).

[9] L. K. Gallos, C. Song, S. Havlin, and H. A. Makse, Proc. Natl. Acad. Sci. U.S.A. **104**, 7746 (2007).

[10] M. C. González, C. A. Hidalgo, and A.-L. Barabási, Nature (London) **453**, 779 (2008).

[11] C. Song, T. Koren, P. Wang, and A.-L. Barabási, Nat. Phys. **6**, 818 (2010).

[12] E. López, S. V. Buldyrev, S. Havlin, and H. E. Stanley, Phys. Rev. Lett. **94**, 248701 (2005).

[13] S. Carmi, Z. Wu, E. López, S. Havlin, and H. E. Stanley, Eur. Phys. J. B **57**, 165 (2007).

[14] S. Carmi, Z. Wu, S. Havlin, and H. E. Stanley, EPL **84**, 28005 (2008).

[15] G. Li, L. A. Braunstein, S. V. Buldyrev, S. Havlin, and H. E. Stanley, Phys. Rev. E **75**, 045103 (2007).

[16] J. D. Noh and H. Rieger, Phys. Rev. Lett. **92**, 118701 (2004).

[17] L. K. Gallos, Phys. Rev. E **70**, 046116 (2004).

[18] E. M. Bollt and D. ben Avraham, New J. Phys. **7**, 26 (2005).

[19] A. Baronchelli, M. Catanzaro, and R. Pastor-Satorras, Phys. Rev. E **78**, 011114 (2008).

[20] R. Carvalho, L. Buzna, F. Bono, E. Gutiérrez, W. Just, and D. Arrowsmith, Phys. Rev. E **80**, 016106 (2009).

[21] S. R. Yu, M. Burkhardt, M. Nowak, J. Ries, Z. Petrášek, S. Scholpp, P. Schwille, and M. Brand, Nature (London) **461**, 533 (2009).

[22] K. C. Leptos, J. S. Guasto, J. P. Gollub, A. I. Pesci, and R. E. Goldstein, Phys. Rev. Lett. **103**, 198103 (2009).

[23] E. W. Montroll and G. H. Weiss, J. Math. Phys. **6**, 167 (1965).

[24] H. Scher and E. W. Montroll, Phys. Rev. B **12**, 2455 (1975).

[25] J. Klafter and R. Silbey, Phys. Rev. Lett. **44**, 55 (1980).

[26] R. Metzler and J. Klafter, Phys. Rep. **339**, 1 (2000).

[27] B. Berkowitz and H. Scher, Phys. Rev. Lett. **79**, 4038 (1997).

[28] M. Dentz, H. Scher, D. Holder, and B. Berkowitz, Phys. Rev. E **78**, 041110 (2008).

[29] M. Molloy and B. Reed, Random Struct. Algorithms **6**, 161 (1995).

[30] W. Aiello, F. Chung, and L. Lu, in *Proceedings of the 32nd Annual ACM Symposium on Theory of Computing* (ACM, Portland, OR, 2000).

[31] A. Tero, S. Takagi, T. Saigusa, K. Ito, D. P. Bebber, M. D. Fricker, K. Yumiki, R. Kobayashi, and T. Nakagaki, Science **327**, 439 (2010).

[32] A. F. Rozenfeld, R. Cohen, D. ben-Avraham, and S. Havlin, Phys. Rev. Lett. **89**, 218701 (2002).

[33] G. Li, S. D. S. Reis, A. A. Moreira, S. Havlin, H. E. Stanley, and J. S. Andrade, Jr., Phys. Rev. Lett. **104**, 018701 (2010).

[34] B. Berkowitz, A. Cortis, M. Dentz, and H. Scher, Rev. Geophys. **44**, RG2003 (2006).

[35] M. F. Shlesinger, J. Stat. Phys. **10**, 421 (1974).

[36] A reviewer suggested that the scaling $w(\tau) = d\tau^{-2}\Phi(d/\tau) \sim \tau^{\gamma-1}$ [where $\Phi(u)$ is the velocity distribution] captures the *increasing* portion of the waiting time distribution, corresponding to early times [Fig. 5(a)]. Indeed, to first approximation, this scaling is consistent with the simulation results.